From classical four-wave mixing to parametric fluorescence in silicon microring resonators

Stefano Azzini,[1] Davide Grassani,[1] Matteo Galli,[1] Lucio Claudio Andreani,[1] Marc Sorel,[2] Michael J. Strain,[2] L. G. Helt,[3] J. E. Sipe,[3] Marco Liscidini,[1] and Daniele Bajoni[4,*]

[1]*Dipartimento di Fisica, Università degli Studi di Pavia, via Bassi 6, Pavia, Italy*

[2]*School of Engineering, University of Glasgow, Glasgow G12 8LT, UK*

[3]*Department of Physics and Institute for Optical Sciences, University of Toronto, 60 St. George Street, Toronto, Ontario M5S 1A17, Canada*

[4]*Dipartimento di Ingegneria Industriale e dell'Informazione, Università degli Studi di Pavia, via Ferrata 1, Pavia, Italy*

**Corresponding author: daniele.bajoni@unipv.it*

Received June 22, 2012; revised August 3, 2012; accepted August 3, 2012;
posted August 6, 2012 (Doc. ID 171082); published September 7, 2012

Four-wave mixing (FWM) can be either stimulated or occur spontaneously. The first process is intrinsically much stronger and well understood through classical nonlinear optics. The latter, also known as parametric fluorescence, can be explained only in the framework of a quantum theory of light. We experimentally demonstrated that, in a microring resonator, there is a simple relation between the efficiencies of these two processes that is independent of the nonlinearity and ring size. In particular, we have shown the average power generated by parametric fluorescence can be immediately estimated from a classical FWM experiment. These results suggest that classical nonlinear characterization of a photonic integrated structure can provide accurate information on its nonlinear quantum properties.

OCIS codes: 130.4310, 270.1670, 250.4390.

Microring resonators have been investigated for more than a decade, with applications ranging from signal processing to optical sensing [1,2]. These resonators are extremely appealing for on-chip integrated optics and are already used in commercial devices because they can be realized following CMOS-compatible processes in silicon [3], silicon nitride [4], or hydex [5,6].

The large field intensity that can be obtained by constructive interference within the ring has inspired several theoretical proposals and experiments in nonlinear optics, including nonlinear bistability [3], parametric frequency conversion [5,7,8], parametric fluorescence [9], and frequency comb generation [4,6]. In this regard, four-wave mixing (FWM) is probably the most investigated process. It is a third-order nonlinear effect that can be viewed as the elastic scattering of two photons of a beam (pump), which results in the generation of two new photons at different frequencies (idler and signal) [10]. This nonlinear effect can occur with (stimulated FWM) or without (spontaneous FWM) an input signal beam. Spontaneous FWM, also known as parametric fluorescence, is particularly interesting, because it can be exploited for the generation of correlated photon pairs [11] used to construct qubits in quantum information and quantum computation.

For a given device, there is obviously a connection between the efficiencies of spontaneous and classical FWM, as the two processes originate from the same material nonlinearity. Thus, it is expected that systems designed to enhance stimulated FWM can be used to generate correlated photon pairs. Yet, it would be extremely helpful to know the efficiency of spontaneous FWM in a device from nonlinear characterization via stimulated FWM [12]. The stimulated process is indeed intrinsically much more efficient, and thus can be observed more easily.

In this work, we studied stimulated and spontaneous FWM in microring resonators and investigated their efficiencies with respect to the characteristic parameters of the ring: the radius R and the resonance quality factor Q. We considered single-channel, side-coupled ring resonators. In this system, for any triplet of resonances equally separated in energy, assuming $\omega_s \simeq \omega_p \simeq \omega_i$, and considering a similar Q and group velocity v_g, the generated powers integrated over the idler resonance are

$$P_{i,\mathrm{ST}} = (\gamma 2\pi R)^2 \left(\frac{Q v_g}{\omega_p \pi R}\right)^4 P_s P_p^2, \tag{1}$$

and

$$P_{i,\mathrm{SP}} = (\gamma 2\pi R)^2 \left(\frac{Q v_g}{\omega_p \pi R}\right)^3 \frac{\hbar \omega_p v_g}{4\pi R} P_p^2, \tag{2}$$

for the stimulated and spontaneous processes, respectively [13]. These expressions can be calculated following [14], assuming the critical coupling condition for the CW pump of power P_p, tuned to the central resonance, and considering, in the stimulated case, a CW signal of power P_s tuned to the lowest energy resonance. Here γ is the nonlinear parameter of the ring waveguide [11]. It is interesting that, given the same input pump power P_p, the ratio between spontaneous and stimulated powers

$$\frac{P_{i,\mathrm{SP}}}{P_{i,\mathrm{ST}}} = \frac{1}{4Q} \frac{\hbar \omega_p^2}{P_s}, \tag{3}$$

is independent of the ring size, but it depends uniquely on the resonance quality factor, the signal power in

the stimulated experiment, and a characteristic power $\hbar\omega_p^2$. For example, at $\hbar\omega_p = 0.8$ eV, we have $\hbar\omega_p^2 \simeq 160$ μW. This makes it possible, given Q, to determine the number of pairs generated in the quantum process solely by means of the corresponding stimulated FWM experiment, once the value of Q is known.

The devices were fabricated on a silicon-on-insulator (SOI) wafer via e-beam lithography and inductively coupled plasma etching. Rings with radii of 5, 10, 20, and 30 μm were side-coupled to a single bus waveguide: The waveguides and rings have a 220×500 nm^2 rectangular cross section. Spot-sized converters are used for efficient coupling [15]. The silicon chip was finally coated with a protective polymethyl methacrylate (PMMA) layer. The samples were characterized using a swept laser and a transmission curve for $R = 5$ μm is shown in Fig. 1. The spectrum shows distinct resonances (Q~7900) with the transmission falling to less than 1%, a sign that the ring is in critical coupling with the access waveguide. In the other samples, the Q factors are Q~8400 for $R = 10$ μm, Q~12000 for $R = 20$ μm and Q~15000 for $R = 30$ μm [16].

For the nonlinear experiment, a tunable laser (Santec TSL-510) set at the pump and, for the stimulated FWM experiments, another set at the signal frequencies, were injected into the bus waveguide of the rings with a tapered lensed fiber. The emitted light was spectrally filtered and sent to a CCD detector. Figure 2 shows the results of FWM experiments on the $R = 5$ μm ring resonator, the sample with the smallest footprint, using the resonances marked in Fig. 1. The power coupled into the ring and generated within the ring are estimated by measuring the losses of each component of the experimental setup and consequently rescaling the output power from the laser or the power measured by the CCD (which was calibrated before the experiment). Coupling losses to and from the sample are obtained as half its total insertion loss (measured to be about 7 dB). We evaluated a total error of about 10% on the estimated powers. Figure 2(a) shows an example of spontaneously generated signal and idler beams. The widths of the peaks are identical to those measured in transmission experiments, indicating that there is little degradation from free carrier absorption. The integrated intensities for the signal and idler beams for spontaneous FWM, as well as the integrated intensity of the idler beam for stimulated FWM at fixed signal input power ($P_s = 200$ μW), are shown in Fig. 2(b) as a function of P_p. In all cases, the intensities follow the expected quadratic dependence of Eqs. (1) and (2). Notice that the saturation observed for $P_p > 2$ mW is due to the thermo-optic effect induced by two-photon absorption, which produces a small redshift of the ring resonances [3,17]. We have also verified that, inclassic FWM, the idler intensity scales linearly with P_s.

We performed a best fit of the stimulated FWM data [black dashed curve in Fig. 2(b)] using γ as the only fit parameter. We took $v_g = c/n_{\text{eff}}$, where $n_{\text{eff}} = 2.47$ is estimated by numerical simulation and is a typical mode effective index for this kind of waveguide [8], obtaining $\gamma = 190$ W^{-1} m^{-1}, a value consistent with those already

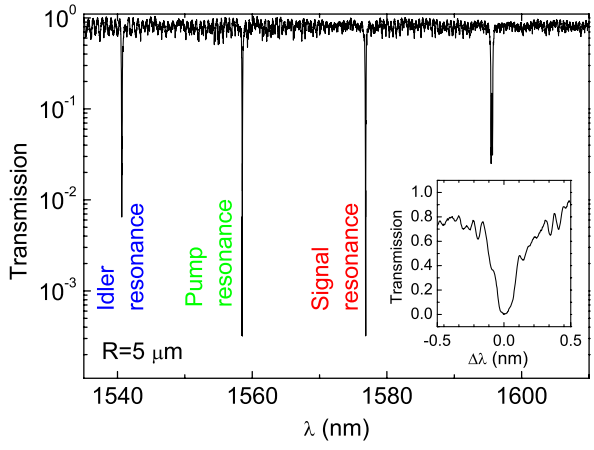

Fig. 1. (Color online) Transmission spectrum of the $R = 5$ μm ring. The inset shows a high-resolution spectrum of the resonance at 1558.5.

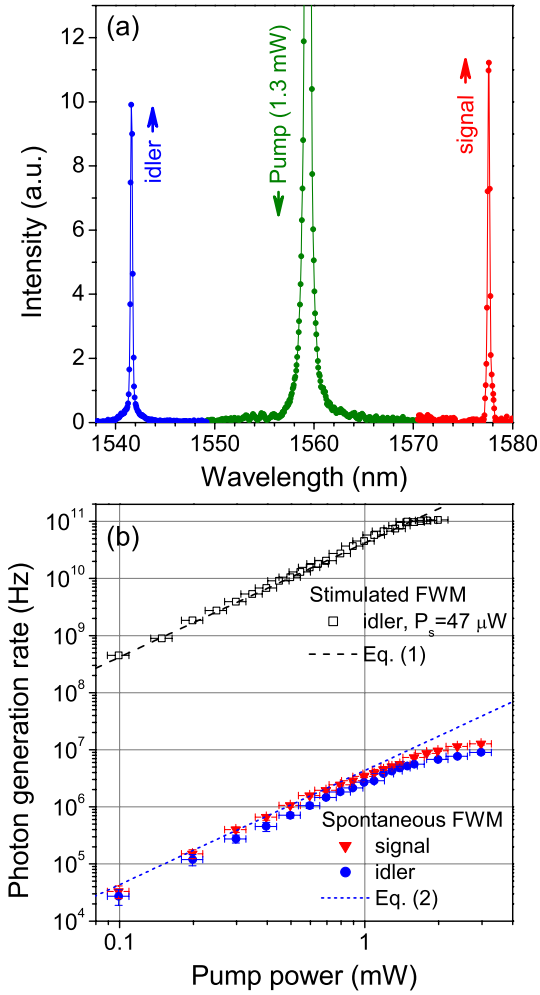

Fig. 2. (Color online) (a) Example of a spontaneous FWM spectrum for a $R = 5$ μm ring resonator. (b) Scaling of the estimated number of generated signal (blue circles) and idler (red triangles) photons inside the ring for spontaneous FWM with varying P_P. It is the same for idler photons in classical FWM (black squares), with 47 μW injected at the signal resonance. The black dashed line is the best fit to the stimulated data from Eq. (1) and the blue short dashed line is the theoretical prediction from Eq. (2).

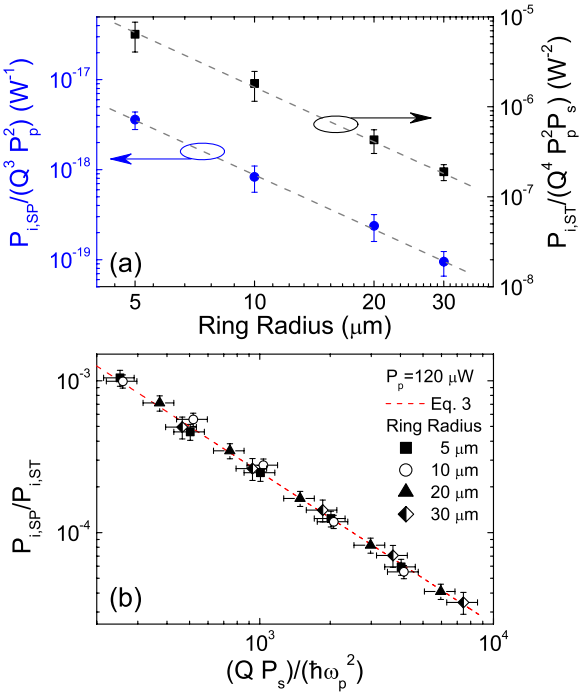

Fig. 3. (Color online) (a) Scaling of the generated idler intensities with the ring radius, for stimulated and spontaneous processes. The dashed lines are guides to the eye proportional to R^{-2}. (b) Ratio between the generated idler photons in spontaneous and classical processes [see Eq. (3)] for all the four rings investigated. The dashed line is given by Eq. (3).

reported in [8]. We then used this value to compute the expected spontaneous emission rate using Eq. (2). The result is shown as a short dashed blue line in Fig. 2(b), which is in good agreement with the experiments.

FWM experiments were carried out on rings with radii of 5, 10, 20 and 30 μm to verify the scaling of Eqs. (1), (2), and (3) with R. In all cases, we chose rings near the critical coupling condition and worked with the same separation in energy between the signal, pump, and idler resonances: This means we chose the first neighbors in the case of the $R = 5$ μm ring [Fig. 1(b)], second neighbors for $R = 10$ μm, fourth neighbors for $R = 20$ μm, and sixth neighbors for $R = 30$ μm. In Fig. 3(a), we have shown stimulated and spontaneous idler powers as a function of R: The data were averaged on a set of measurements varying P_p and P_s. Notice that, for all data of Fig. 3, we kept $P_p < 1$ mW to avoid the thermo-optic effect. As expected from Eqs. (1) and (2), both of the generated powers scale as R^{-2}. Finally, in Fig. 3(b) we have shown the ratio between the measured generated idler powers in the spontaneous and in the classical processes as a function of $Q \cdot P_s$. The data show an excellent agreement with Eq. (3) and confirm that the ratio is independent of the ring radius. More importantly, these results prove that data from stimulated FWM can be used to precisely predict spontaneous FWM generation rates. For clarity, in Fig. 3(b) we show only data for $P_p = 0.12$ mW, but we obtained the same results for all the investigated pump powers varying between 60 μW and 1 mW.

In conclusion, we have reported classical and spontaneous FWM in silicon microring resonators. We have verified that the efficiency of the spontaneous process is related to that of the classical process by a simple analytical formula. This result is of interest because it is general and not limited to ring resonators [14]. Given any photonic structure, the application of this method allows the derivation of the number of photon pairs generated in the spontaneous process through a simple measure of the classical process, greatly simplifying the characterization of any structure designed for the generation of quantum photonic states.

This work was supported by the Italian Ministry of Education, University and Research (MIUR) funding through the Investment Fund of Basic Research (FIRB) Futuro in Ricerca project RBFR08XMVY and from the Alma Mater Ticinensis Foundation.

References and Notes

1. B. Little, S. Chu, and H. Haus, Opt. Lett. **23**, 1570 (1998).
2. J. Robinson, L. Chen, and M. Lipson, Opt. Express **16**, 4296 (2008).
3. V. R. Almeida and M. Lipson, Opt. Lett. **29**, 2387 (2004).
4. J. S. Levy, A. Gondarenko, M. A. Foster, A. C. Turner-Foster, A. L. Gaeta, and M. Lipson, Nature Photon. **4**, 37 (2010).
5. M. Ferrera, L. Razzari, D. Duchesne, R. Morandotti, Z. Yang, M. Liscidini, J. E. Sipe, S. Chu, B. E. Little, and D. J. Moss, Nature Photon. **2**, 737 (2008).
6. L. Razzari, D. Duchesne, M. Ferrera, R. Morandotti, S. Chu, B. E. Little, and D. J. Moss, Nature Photon. **4**, 41 (2010).
7. P. P. Absil, J. V. Hryniewicz, B. E. Little, P. S. Cho, R. A. Wilson, L. G. Joneckis, and P.-T. Ho, Opt. Lett. **25**, 554 (2000).
8. A. Turner, M. Foster, A. Gaeta, and M. Lipson, Opt. Express **16**, 4881 (2008).
9. S. Clemmen, K. Phan Huy, W. Bogaerts, R. G. Baets, Ph. Emplit, and S. Massar, Opt. Express **17**, 16558 (2009).
10. R. W. Boyd, *Nonlinear Optics*, 3rd ed. (Academic, 2008).
11. L. G. Helt, Z. Yang, M. Liscidini, and J. E. Sipe, Opt. Lett. **35**, 3006 (2010).
12. L. G. Helt, M. Liscidini, and J. E. Sipe, J. Opt. Soc. Am. B **29**, 2199 (2012).
13. Unlike in Ref. [12], here we assume losses in the ring resonator. At the critical coupling, the on-resonance field enhancement in the ring resonator is $\mathrm{FE} \simeq \sqrt{\frac{2Qv_g}{\omega_0 L}}$, with ω_0 the resonant frequency (see also Ref. [7]).
14. M. Liscidini, L. G. Helt, and J. E. Sipe, Phys. Rev. A **85**, 013833 (2012).
15. M. Notomi, A. Shinya, S. Mitsugi, E. Kuramochi, and H.-Y. Ryu, Opt. Express **12**, 1551 (2004).
16. The variation of the quality factor between the signal, pump, and idler resonances is below 2% for all four rings. The value we have taken for the quality factor in the equations is an average between the Qs of the three resonances.
17. We verified that the quadratic trend is maintained up to the maximum available pump power if the pump wavelength is retuned to compensate for the thermo-optic redshift of the resonances for $P_p > 2$ mW. This implies that Q degradation due to free carrier absorption can be neglected for all the investigated P_p. The data of Fig. 2 are taken with a fixed value of the pump energy.